ARTICLE

An X-Linked Myopathy with Postural Muscle Atrophy and Generalized Hypertrophy, Termed XMPMA, Is Caused by Mutations in *FHL1*

Christian Windpassinger,[1,2,*] Benedikt Schoser,[3] Volker Straub,[4] Sonja Hochmeister,[5] Abdul Noor,[1] Birgit Lohberger,[5] Natalie Farra,[1] Erwin Petek,[2] Thomas Schwarzbraun,[2] Lisa Ofner,[2] Wolfgang N. Löscher,[6] Klaus Wagner,[2] Hanns Lochmüller,[3] John B. Vincent,[1] and Stefan Quasthoff[5]

We have identified a large multigenerational Austrian family displaying a novel form of X-linked recessive myopathy. Affected individuals develop an adult-onset scapulo-axio-peroneal myopathy with bent-spine syndrome characterized by specific atrophy of postural muscles along with pseudoathleticism or hypertrophy and cardiac involvement. Known X-linked myopathies were excluded by simple-tandem-repeat polymorphism (STRP) and single-nucleotide polymorphism (SNP) analysis, direct gene sequencing, and immunohistochemical analysis. STRP analysis revealed significant linkage at Xq25–q27.1. Haplotype analysis based on SNP microarray data from selected family members confirmed this linkage region on the distal arm of the X chromosome, thereby narrowing down the critical interval to 12 Mb. Sequencing of functional candidate genes led to the identification of a missense mutation within the four and a half LIM domain 1 gene (*FHL1*), which putatively disrupts the fourth LIM domain of the protein. Mutation screening of FHL1 in a myopathy family from the UK exhibiting an almost identical phenotype revealed a 3 bp insertion mutation within the second LIM domain. *FHL1* on Xq26.3 is highly expressed in skeletal and cardiac muscles. Western-blot analysis of muscle biopsies showed a marked decrease in protein expression of FHL1 in patients, in concordance with the genetic data. In summary, we have to our knowledge characterized a new disorder, X-linked myopathy with postural muscle atrophy (XMPMA), and identified *FHL1* as the causative gene. This is the first FHL protein to be identified in conjunction with a human genetic disorder and further supports the role of FHL proteins in the development and maintenance of muscle tissue. Mutation screening of *FHL1* should be considered for patients with uncharacterized myopathies and cardiomyopathies.

Introduction

Myopathies are inherited muscle disorders characterized by weakness and atrophy of voluntary skeletal muscle, and several types of myopathy also show involvement of cardiac muscle. Different forms of myopathy vary with respect to pattern of inheritance, age of onset, incidence, rate of progression, and finally, distribution and severity of muscle weakness. Several myopathies exhibit an X recessive mode of transmission. Duchenne muscular dystrophy (DMD; Xp21.2; MIM #310200), the most common X-linked myopathy, is mainly caused by frameshift mutations that result in the complete absence of functional dystrophin, whereas the less severe Becker MD (BMD; MIM #300376) is typically associated with missense and in-frame deletions that result in reduced levels of functional dystrophin, or expression of partially functional protein.[1] DMD is correlated with onset before age 6 and a typical life span of 20-25 years; in contrast, BMD has onset in adolescence or adulthood, with symptoms similar to but generally less severe than DMD. Both DMD and BMD present with progressive muscle wasting with limb-girdle distribution, pseudohypertrophy of the calf muscles, and frequently, cardiomyopathy. Emery-Dreifuss MD (EDMD; MIM #310300) is another form of adult-onset X recessive MD caused by deficiencies in the emerin protein, encoded by the *EMD* gene on Xq28.[2] EDMD is phenotypically distinct from other X-linked MDs, with pronounced contractures, rigid spine, a humeroperoneal distribution of muscle wasting, and frequently, cardiomyopathy. X-linked myopathy with excessive autophagy (XMEA; MIM %310440) also maps to Xq28 and shows progressive atrophy of skeletal muscles with no cardiac involvement, and an analysis of biopsied muscle fibers shows excessive autophagy and exocytosis.[3] Finally, an X-linked multisystem disorder, McLeod syndrome, affecting red blood cells, the peripheral and central nervous systems, and skeletal and cardiac muscle, maps to Xp21.2–p21.1 (MIM 314850).[4]

In this study, a large multigenerational Austrian family was identified, and six living affected members were ascertained and examined. Pedigree analysis (Figure 1) is compatible with an X-linked recessive pattern of inheritance. We describe the clinical delineation of a new muscular disease, along with genetic studies to identify the underlying cause and molecular studies to show how the identified gene and encoded protein might contribute to the disease.

In 1971, an affected male member (now deceased) of our large Austrian family was investigated, and a report on this

[1]Neurogenetics Section, The Centre for Addiction and Mental Health, University of Toronto, Toronto, Ontario, M5T 1R8, Canada; [2]Institute of Human Genetics, Medical University of Graz, A-8010 Graz, Austria; [3]Friedrich-Baur Institute, Department of Neurology, Ludwig Maximilians University Munich, 80336 Munich, Germany; [4]Institute of Human Genetics, University of Newcastle upon Tyne, International Centre for Life, Newcastle upon Tyne, NE1 3BZ, UK; [5]Department of Neurology, Medical University of Graz, A-8036 Graz, Austria; [6]Clinical Department of Neurology, Innsbruck Medical University, A-6020 Innsbruck, Austria
*Correspondence: christian.windpassinger@meduni-graz.at
DOI 10.1016/j.ajhg.2007.09.004.

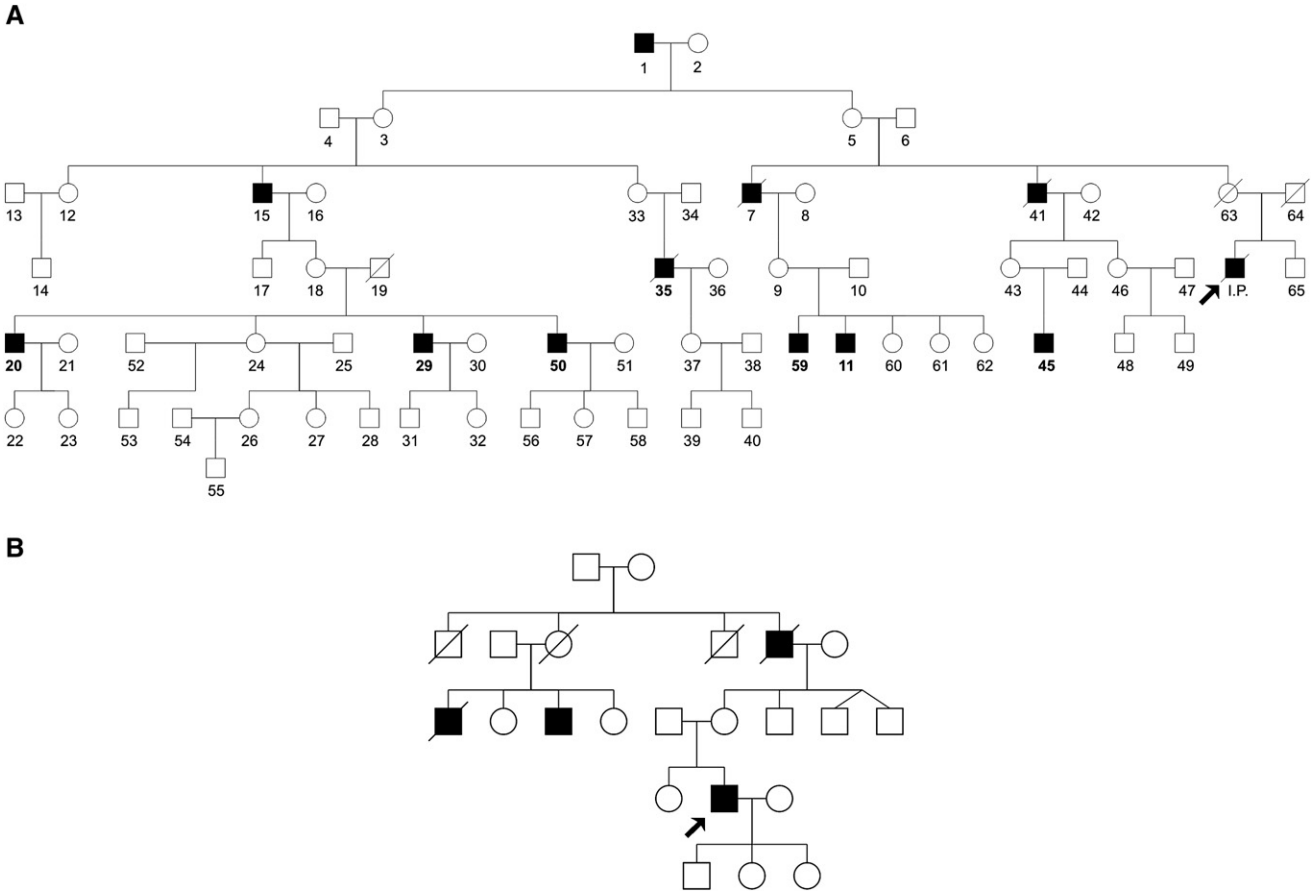

Figure 1. Pedigree of the X-Linked Myopathy with Postural Muscle Atrophy Families
(A) Only the core pedigree is shown here. Affected males are indicated by filled squares. The patient from the Schwarzmeier et al.[5] study is indicated with an arrow.
(B) The second XMPMA family, from the UK, is shown. The index patient is marked with an arrow.

single case was published because the unusual phenotype could not be classified. This patient was reported to show a progressive muscular dystrophy of pelvicofemoral and scapulohumeral type that was different from all other known muscle dystrophies.[5] The muscle pathology had some similarities with myotonic dystrophy 1; however, this was ruled out because no myotonic reaction was observed. Finally, significantly lowered Mg^{2+}-ATPase levels were reported; however, the pathology did not suggest any known metabolic myopathy.

In the extended family of this patient, many members are affected by a distinct form of adult-onset X-linked recessive myopathy with several features in common with other MDs, but the presentation of a pseudoathletic phenotype, scapuloperoneal weakness, and bent spine is unique and might render the clinical phenotype distinguishable from other myopathies. Further, immunohistochemical analysis of muscle tissue revealed no deficiency in proteins associated with known MDs, either autosomal or X-linked, including dystrophin and emerin. On the basis of striking similarities of the unique phenotypical presentation of the Austrian family, we were able to recruit an additional family originating from the UK for our genetic study.

Material and Methods

Clinical Assessment

Probands were identified from a multigenerational Austrian family (Figure 1) displaying clinical features suggesting MD, but with clinical differences from previously described myopathies. Institutional-research ethics-board approval for study of the family was obtained. Patients and family members were recruited after giving informed, written consent. We identified six living patients (all males). Full neurological examination, including nerve conduction velocity (NCV) testing and electromyography (EMG), was performed on all affected individuals included in the study (Table 1). Serum creatine kinase (CK) levels were also measured in affected individuals (Table 1). First-degree relatives were examined when possible, and genealogical data were also collected. Three out of the six patients have been followed up for approximately 5 years for evaluation of disease progression. A second myopathy family, ascertained through the Institute of Human Genetics, Newcastle upon Tyne, UK, was also investigated because of a distinct similarity in symptoms with the Austrian family (Figure 1).

Muscle Biopsy

All muscle specimens were processed with standard histological procedures. One part of the biopsy was embedded in paraffin,

Table 1. Clinical Evaluations for Members of the XMPMA Family from Austria

Patients ID	Age of Onset	CK[a] Level (U/L)	EMG[b]	Muscle MRI[c]	Athletic Habitus in Early Stages	Muscle Biopsy	Cardiac and Lung Involvement	Neck and Achilles Tendons
45	26	620	myopathic	N.D.[d]	yes	N.D.	unknown	unknown
I.P.[e]	30	500-900	myopathic	N.D.	yes	myopathic	cardiomyopathy with arrhythmia	short
20	32	620	N.D.	selective MA,[f] BS[g]	yes	myopathic	hypertrophic cardiomyopathy	short
50	32	400-1774	myopathic	selective MA, BS	yes	myopathic	normal heart evaluation	short
29	30	780	myopathic	–	yes	N.D.	unknown	short
11	30	700	myopathic	selective MA, BS	yes	myopathic	hypertrophic cardiomyopathy	short
59	31	550	myopathic	N.D.	unknown	myopathic	hypertrophic cardiomyopathy	short
35	30	800-1200	myopathic	N.D.	yes	myopathic	respiratory failure	short
I.P UK	35	1300 U/l	normal	N.D.	yes	myopathic	respiratory failure	short

This table includes electromyography, muscle magnetic resonance imaging (MRI), histological examination of biopsied tissue, and involvement of heart and of neck and Achilles tendons. Patients' IDs correspond to numbers given in Figure 1.

[a] CK represents creatine kinase level (normal <170 U/L).

[b] EMG stands for electromyography.

[c] MRI stands for magnetic resonance imaging.

[d] N.D. represents test not done.

[e] I.P. stands for index patient (described in Schwarzmeier et al.[5]).

[f] MA stands for muscle atrophy.

[g] BS stands for bent spine.

and another was frozen in liquid nitrogen. Cryosections (8–10 μm) were stained with hematoxylin and eosin, reduced nicotinamide adenine dinucleotide-tetrazolium reductase, adenosine triphosphatase reactions at pH 4.6 and pH 10.4, modified Gomori trichrome, van Gieson, cytochrome *C* oxidase, succinic dehydrogenase, Sudan black *B*, acid phosphatase, and periodic acid-Schiff.[6]

Magnetic Resonance Imaging

Muscle magnetic resonance imaging (MRI) was performed with a 1.5 Tesla Siemens Avanto system (Graz, Austria). Magnet resonance imaging of the axial and coronal planes of the spine and upper and lower extremities, as well as the shoulder girdles, with conventional T1-weighted spin echo (repetition time TR of 500 ms, echo time TE of 13 ms, with slight variations) and short tau inversion recovery sequences was performed. The slices were 10 mm thick for the lower extremities and 6–10 mm thick for the upper extremities, with an interslice gap of 6–10 mm. The T1-weighted images were evaluated with regard to degree of muscle atrophy (volume loss) and intramuscular fatty infiltration.

Electron Microscopy

Biopsy specimens for electron microscopy were fixed in 6.25% ice-cold glutaraldehyde in Sørensen's 0.1 M phosphate buffer at pH 7.3. After thorough rinsing in buffer, samples were postfixed in 2% buffered osmium tetroxide. After rapid dehydration in graded series of acetone, tissue blocks were embedded in Epon. Semithin sections of the embedded blocks were stained with paraphenylenediamine. Ultrathin sections were contrast enhanced with uranyl acetate and lead citrate and examined with a Philips 400 T transmission electron microscope.

Muscle Immunocytochemistry

We used standard immunocytochemistry protocols to perform staining for dystrophin, adhalin, merosin, dysferlin, caveolin, α-dystroglycan, emerin, lamin A/C, desmin, β-slow myosin heavy chain, spectrin, and α-sarcoglycan after muscle biopsies of patient 50 (Figure 1). Monoclonal antibodies were obtained from Novocastra Laboratories (Vision BioSystems) for spectrin (NCL-SPEC1), dysferlin (NCL-Hamlet), emerin (NCL-Emerin), and α-sarcoglycan (NCL-α-SARC). Additional Novocastra antibodies were used for dystrophin staining, specific to the dystrophin rod-like domain (NCL-DYS1), C terminus (NCL-DYS2), and N terminus (NCL-DYS3). Monoclonal antibodies were employed for merosin (MAB 1922; Chemicon), caveolin (Caveolin3; Transduction Laboratories, BD Biosciences), α-dystroglycan (KlonVIA4-1; Upstate Biotechnology, Europe), lamin A/C (Mouse Hybridoma Supernatant), desmin (M0760, Klon D33; Dako), and myosin (805-502-L001, Lot L02279, Klon A4.951; Alexis Biochemicals) staining procedures.

STRP Analysis

Genomic DNA was extracted from blood samples with standard procedures. DNA was amplified by PCR with conditions adapted from the ABI Prism Linkage Mapping Set v2.5 (MD10) protocol. Denaturation was performed at 95°C for 15 min and then followed by ten cycles of 94°C for 15 s, 55°C for 15 s, and 72°C for 30 s. This was followed by 20 cycles of 89°C for 15 s, 55°C for 15 s, and 72°C for 30 s, with a final extension step of 72°C for 10 min. Reaction mix consisted of 50 ng genomic DNA, 0.1 μmol of each primer, and HotStar *Taq* Master Mix (QIAGEN) in a reaction mix of 10 μL. Haplotype analysis was performed with CYRILLIC v2.1 (Cyrillic Software). Five intragenic STRP markers, DXS1238, DXS1237, DXS997, DXS1236, and DXS1235, were selected for exclusion of the *DMD* gene. The following additional markers spanning the whole X chromosome were selected for linkage analysis: DXS1060, DXS987, DXS1226, DXS1214, DXS1068, DXS993, DXS991, DXS986, DXS990, DXS1106, DXS8055, DXS1001, DXS1047, DXS6854*, DXS8094*, DXS1192*, DXS1232*, DXS1227, DXS8043, DXS8091, and DXS1073 (markers identified with an asterisk were selected from UCSC; all other markers were

from the ABI Prism Linkage Mapping Set MD10). For the UCSC-selected markers, forward primers were labeled at their 5′ ends with either 5-carboxyfluorescein (FAM) or NED fluorochromes. Primer sequences for the STRP markers are available from the UCSC Genome Browser. Products were diluted and size-separated with the ABI 3100 Genetic Analyzer (Applied Biosystems).

Linkage Analysis

Multipoint nonparametric linkage was computed with easyLINKAGE plus v5.02 platform[7] and the ALLEGRO program version 1.2c.[8] Two-point linkage analysis was also performed with easyLINKAGE plus v5.02 and the SuperLink program version 1.5.[9] Allele frequencies were assumed to be equal and disease frequency was set to 0.0001.

Genome-Wide SNP Analysis: Mapping of a New Locus to Xq26–q27

A genome-wide 250K NspI Affymetrix SNP microarray (Affymetrix, CA, USA) analysis was performed on five affected individuals (see Figure 1, pedigree members 20, 29, 50, 11, and 45) and three unaffected relatives (28, 37, and 46), two of whom were obligate carriers (37 and 46), at the Microarray Facility at The Centre for Applied Genomics (Toronto, Canada). SNP microarray gene chip data was subsequently analyzed with dCHIP software.[10]

Sequencing and Mutation Analysis of Candidate Genes

Candidate genes within the Xq25–q27.1 12 Mb critical region were identified via the UCSC genome browser and were selected according to both tissue-expression profile and known function. The following four genes were chosen for mutation screening: *MBNL3*, *VGLL1*, *FGF13*, and *FHL1*. Primers were designed with the Primer3 program, and we used them to amplify all exons of the functional candidate genes by PCR with genomic DNA (primer sequences available on request). PCR products were sequenced with the BigDye Terminator 3.1 Cycle Sequencing Kit (Applied Biosystems). Sequencing reactions were size-separated on the ABI Prism 3100 DNA Analyzer (Applied Biosystems), and sequence data was collected with the ABI Data Collection software version 1.1 and subsequently analyzed with the ABI DNA Sequencing Analysis version 3.6 software.

Immunohistology

Specimens of vastus-lateralis-muscle and anterior-tibial-muscle biopsy (subjects 50 [vastus lat] and 11 [tib ant] from pedigree in Figure 1) were used for colocalization studies of FHL1 and myosin slow fiber staining by indirect immunofluorescence. In brief, after fixation with 2% para-formaldehyde, blocked with 4% BSA in PBS, samples were combine stained with a polyclonal anti-rabbit FHL1 antiserum (dilution 1:1000 AVIVA Systems Biology) and monoclonal anti-mouse skeletal slow myosin antiserum (dilution 1:5000, Sigma, Germany) overnight at 4°C temperature. After rinsing for 15 min in PBS, the sections were incubated with Cy3-conjugated streptavidin goat anti-rabbit serum (Jackson-Immuno Research, dilution 1:1000) and with Alexa-Fluor 488 goat anti-mouse serum (Invitrogen). After the sections were mounted onto slides, a Leica epifluorescent microscope with a Zeiss Axiovert imaging system was used for visualization. For comparison normal controls, as well as limb-girdle muscular-dystrophy muscle, sections were investigated with identical procedures as described above. Negative controls with omission of the primary antibody did not show any staining.

Immunohistochemistry on cultured muscle cells: primary myoblast cultures of vastus lateralis muscle and anterior tibial muscle specimen (patients 50 and 11), and controls were used for FHL1 staining by indirect immunofluorescence techniques. In brief, after fixation with 2% para-formaldehyde and blocking with 4% BSA in PBS, samples were stained with a polyclonal rabbit FHL1 antiserum (dilution 1:1000 AVIVA Systems Biology) for 1 hr at room temperature. After rinsing for 15 min in PBS, the sections were incubated with Cy3-conjugated goat anti-rabbit serum (Jackson-Immuno Research, West Grove, PA, USA, dilution 1:1000). After the sections were mounted onto slides, a Leica epifluorescent microscope with a Zeiss Axiovert imaging system was used for visualization. Negative controls with omission of the primary antibody did not show any staining.

Western Analysis

For western-blot studies, proteins were extracted from 50 mg of skeletal muscle from five normal controls, five disease controls (Becker MD), and two male patients (50 and 11). Protein concentrations of the supernatants were measured with the BCA Protein Assay Kit (Pierce). Samples were stored frozen at 80°C. Aliquots of protein (2 μg) were loaded onto a sodium dodecyl sulfate (SDS)-polyacrylamide gel, composed of 4% stacking (0.5 M Tris-HCL [pH 6.8] and 10% SDS) and 10% resolving (1.5 M Tris-HCL [pH 8.8] and 12% SDS) gels. The protein was then transferred to nitrocellulose membranes (Schleicher and Schuell) for 1 hr (110V). Nonspecific binding was blocked for 2 hr with TBST (10 mM Tris-HCL [pH 7.4], 140 mM NaCl, and 0.1% Tween-20) containing 5% skimmed milk; this was followed by incubation with primary antibodies for 4 hr at room temperature. Rabbit polyclonal antibody anti-FHL1 (AVIVA Systems Biology) was used at a dilution of 1:2000 in TBST-5% skim milk. After washing, the membranes were incubated with the corresponding anti-rabbit or anti-mouse IgG secondary antibodies (Dako) at a dilution of 1:1000 for 1 hr at room temperature. The membranes were developed with the chemiluminescence ECL system (Pharmacia) and then exposed to autoradiographic film. Analysis of immunoreactive bands was performed semiquantitatively. Blots were stripped and blots reincubated with mouse monoclonal anti-adhalin antibody (Novocastra) at a dilution of 1: 2000.

Alignment of LIM-Domain Sequence

Alignment of homologous amino acid sequences for the FHL1 fourth LIM domain was performed with the BOXSHADE program, with sequences from human (NP_001440), orangutan (CAH91622), rhesus monkey (XP_001103233), pig (NP_999540), mouse (NP_034341), opossum (XP_001379179), platypus (translated from platypus genomic Contig9.330), chicken (XP_001234114), zebrafish (XP_001334290), *Xenopus tropicalis* (NP_001006703), and *tetraodon nigroviridis* (CAF92807).

Results

Clinical Assessment

Austrian Family

Clinical assessment in all six patients as well as two now-deceased patients from this family (Figure 1A) revealed a unique and characteristic phenotype (Table 1). During the early stages of disease, all subjects showed an athletic

appearance (Figure 2); however, detailed examination revealed weakness and atrophy of postural muscles, whereas other muscles appeared hypertrophic. Affected (atrophied) muscles included the soleus, peroneus longus, tibialis anterior, vastus medialis, biceps femoris, erector spinae, and the lower part of the latissimus dorsi. A list of muscle groups that were atrophic, hypertrophic, or normal in affected individuals is given in Table 2 and shows that muscles with predominantly type I fiber content are generally atrophic, whereas muscles with predominantly type II fibers are generally hypertrophic. Moreover, a mild scapular winging was noted in all patients, to complete a scapulo-axio-peroneal syndrome. Additionally, all patients had significant contractures of the Achilles tendon and hamstrings, a short neck, and also a mechanically limited range of neck flexion and extension analogous to bent-spine syndrome. Tendon reflexes, sensory examination, and mental status were normal. In all affected individuals scoliosis, back pain, gait problems, and elevated creatine kinase levels were noted (Table 1). Symptoms were not noted until ~30 years, and, in six affected deceased family members, there was a wide range in age of death (45–72 years), typically from heart failure but of unknown mechanism. However, hypertrophic cardiomyopathy was suspected from earlier echocardiographic investigation. Four- to five-year follow up of three of the six affected patients showed an interindividually variable but slow progression of the disease.

UK Family

A second family, of British origin, with a putative diagnosis of Becker muscular dystrophy was identified (Figure 1B). The index patient presented initially with symptoms of hip-flexor weakness (MRC 4) and elevated serum CK levels of ~1300 U/l at the age of 35 years. At that time, he was playing competitive football and showed a very athletic habitus. Muscle hypertrophy was most prominent in his shoulder girdle and arm muscles. Neck flexion was compromised by spinal rigidity. His lung function showed a FVC of 4.6 l (90%) in a sitting position and dropped to 4.0 l (78%) in a lying position. There were no additional clinical signs or symptoms of an underlying skeletal muscle or heart disease. Nerve-conduction studies and an EMG were normal. A muscle biopsy from the vastus lateralis showed type I fiber atrophy, variation in fiber size, with some measuring up to 125 μm in diameter, and a few necrotic fibers. Immunohistochemical and western-blot analysis for proteins of the dystrophin glycoprotein complex, emerin, dysferlin, caveolin, and calpain were normal. Mutation analysis of the genes for dystrophin and emerin did not reveal any abnormalities. The maternal grandfather of the index patient started to experience difficulties with walking at 42 years of age and used a wheelchair for the last years of his life. He died of respiratory failure at 52 with the label of Becker muscular dystrophy. Two nephews of the grandfather were also labeled as Becker muscular dystrophy and experienced slowly progressive muscle weakness in legs and arms from their early 40s. One of the nephews died in his 50s of respiratory failure.

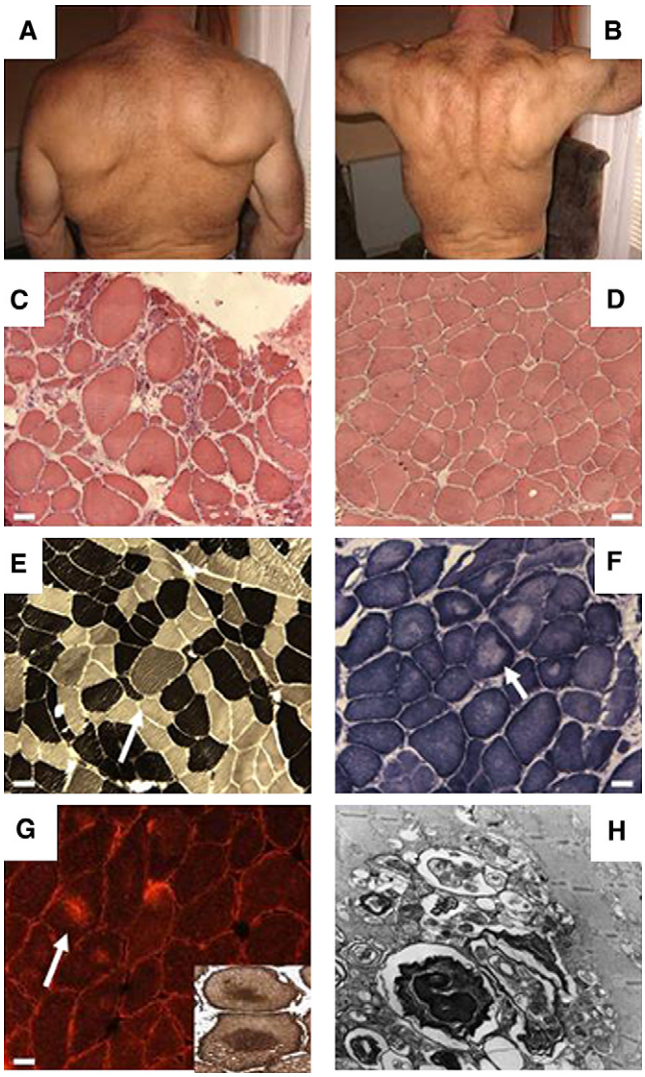

Figure 2. Phenotype and Histological Findings of Patient 20
The clinical phenotype is composed of a scapulo-axio-peroneal syndrome with an athletic appearance. Predominant shoulder girdle atrophy with scapular winging and axial muscular atrophy of postural muscles is found in the patients (A and B). Muscle biopsies show moderate degenerative myopathy. In addition, a few round autophagic vacuolar changes are apparent. H & E stain is shown in (C) and (D). ATPase (pH. 9.4) is shown in (E). Increase in fiber-size variation with hypertrophy of type 2 fibers (arrow in [E]) and atrophy of both fiber types is seen (dark stained fibers correspond to type 2 fibers). In the NADH staining (F), some core-like NADH-negative central zones are seen (arrow in [F]). Immunohistology with monoclonal antibodies against desmin (G) of specimens from patient 50 showed positive staining in core-like lesions (arrow and insert in [G]), and some subsarcolemmal desmin accumulation. Electron microscopy of the muscle from patient 1 shows an autophagic vacuole with autophagic debris including myelin-like figures (H). White scale bars in (C)–(G) adjusted to 30 μm. Magnification × 3300 is shown in (H).

Histological Analysis

Muscle histology revealed a moderate degenerative myopathy with a moderate perimysial and limited endomysial

Table 2. Muscle Involvement in XMPMA Patients

Muscle	Average Muscle-Fiber Composition				
	Type I	Type II	Atrophic	Hypertrophic	Normal
Abductor digiti minimi	51.8	48.2			X
Abductor pollicis brevis	*63.0*	*37.0*			X
Abductor hallucis					X
Adductor magnus (Deep)	*63.3*	*36.7*	*X*		
Biceps brachii (Surface)	42.3	57.7		X	
Biceps brachii (Deep)	50.5	49.5		X	
Biceps fernoris	*66.9*	*33.1*	*X*		
Brachioradialis	39.8	60.2			X
Deltoideus (Surface)	53.3	46.7	X		
Deltoideus (Deep)	*61.0*	*39.0*	*X*		
I dorsal interosseus	57.4	42.6			X
Erector spinae (Surface)	58.4	41.6	X		
Erector spinae (Deep)	54.9	45.1	X		
Extensor digitorum	47.3	52.7		X	
Extensor digitorum brevis	45.3	54.7		X	X
Flexor digitorum brevis	44.5	55.5		X	
Flexor digitorum profundus	47.3	52.7		X	
Gastrocnemius (Lateral head, surface)	43.5	56.5	X		
Gastrocnemius (Lateral head, deep)	50.3	49.7	X		
Gastrocnemius (Medial head)	50.8	49.2	X		
Gluteus medius					X
Gluteus maximus	52.4	47.6			X
Iliocostalis			X		
Interspinales cervicis			X		
Infraspinatus	45.3	54.7		X	
Longus capitis					X
Longus colli					X
Longisimus dorsi			X		
Latissimus dorsi	50.5	49.5			X
Multifidus			X		
Orbicularis oculi	15.4	84.6			X
Obliqus capitis			X		
Peronaeus longus	*62.5*	*37.5*	*X*		
Psoas					X
Rectus abdominis	46.1	53.9		X	
Rectus femoris (Lateral head, surface)	29.5	10.5			X
Rectus femoris (Lateral head, deep)	42.0	58.0			X
Rectus femoris (Medial head)	42.8	57.2			X
Rhomboideus	44.6	55.4		X	X
Semimembranosus			X		
Semispinalis			*X*		
Soleus (Surface)	*86.4*	*13.6*	*X*		
Soleus (Deep)	*89.0*	*11.0*	*X*		
Splenius					X
Sternocleidomastoideus	35.2	64.8		X	X
Supraspinatus	59.3	40.7	X		
Temporalis	46.5	53.5			X
Tibialis anterior (Surface)	*73.4*	*26.6*	*X*		
Tibialis anterior (Deep)	*72.7*	*27.3*	*X*		
Trapezius	53.7	46.2	X		X
Triceps surae			X		
Triceps (Surface)	32.5	67.5		X	
Triceps (Deep)	32.7	67.3		X	
Vastus lateralis (Surface)	37.8	62.2		X	
Vastus lateralis (Deep)	46.9	53.1	X		
Vastus medialis (Surface)	43.7	56.3			X
Vastus medialis (Deep)	*61.5*	*38.5*	*X*		

This table was adapted from Johnson et al.[29] and indicates (by "X") whether, by clinical examination of all six living patients as well as by MRI of three patients in progressed stages of disease, abnormality is present, either atrophic or hypertrophic. Muscles represented in italics normally display significantly high portion of type I muscle fibers; however, in the XMPMA patients, the postural muscles—adductor magnus, biceps femoris, deltoideus, peronaeus longus, soleus, tibialis anterior, and vastus medialis—showed gradual atrophy, whereas many muscles with a high percentage of fiber type II show mild to pronounced hypertrophy.

Table 3. Haplotype Analysis of the DMD Locus in Patients from the Austrian Family

	20	29	50	11	45	46
Marker	Allele Sizes (bp)					
DXS1238	206	206	206	184	184	184/184
DXS1237	178	178	178	178	178	174/178
DXS997	115	115	115	115	115	107/113
DXS1236	251	233	233	239	235	233/239
DXS1235	245	245	245	245	245	233/235

Genotypes are given for patients 20, 29, 50, 11, and 45 (shaded) as well as obligate carrier 46 (unshaded) (see Figure 1).

Table 4. Two-Point Linkage Analysis

Marker	POS_cM	0	0.1	0.2	0.3	0.4
DXS986	57.383	−17.6293	−1.5459	−0.8108	−0.4359	−0.1914
DXS990	60.622	−8.8048	−0.2483	0.0654	0.1219	0.079
DXS1106	68.742	−3.9435	0.8234	0.8123	0.6214	0.3395
DXS8055	70.911	−3.9537	0.5575	0.7252	0.6068	0.3481
DXS1001	75.791	1.9488	1.6479	1.2864	0.8843	0.4532
DXS1047	82.844	2.4266	2.0061	1.5388	1.0339	0.5078
DXS6854	82.8445	2.8794	2.3985	1.8633	1.2768	0.6483
DXS8094	82.854	3.3472	2.7653	2.1348	1.4531	0.7292
DXS1192	83.921	3.4417	2.8448	2.1943	1.4892	0.7434
DXS1232	85.55	2.5869	2.1928	1.7225	1.1925	0.6147
DXS1227	88.33	−13.9949	0.111	0.2855	0.2194	0.1025
DXS8043	94.221	−4.4146	0.7774	0.7002	0.4955	0.2517
DXS8091	97.891	−10.8139	0.3899	0.4965	0.3574	0.1628
DXS1073	102.351	−16.1018	−1.123	−0.3448	−0.0628	0.0203

This table shows linkage data for X chromosome STRPs, analyzed with the SuperLink program version 1.5[9] from easyLINKAGE plus v5.02. Allele frequencies were assumed to be equal, and disease frequency was set to 0.0001. Positions of markers are indicated in centimorgans (cM), as provided by Marshfield. LOD scores for theta values of 0, 0.1, 0.2, 0.3, and 0.4 are shown. Significant LOD scores (>2) are shaded with dark gray, and positive LOD scores are shaded with light gray.

fibrosis. Centrally placed myonuclei were increased, and rarely single-fiber necrosis and granular myofiber degeneration were seen (fiber-size variation was increased in all specimens with diameters ranging between 20 and 120 μm; see Figure 2), and most prominent in type 2 fibers. A few autophagic vacuoles predominant in type 2 fibers were detectable (Figure 2). In NADH and COX histochemistry, centrally negative core-like lesions were detected (Figure 2), without any further mitochondrial alterations. Electron microscopy revealed autophagic vacuoles with myelin-like debris (Figure 2). Immunohistology showed pronounced antidesmin staining in the core-like zones (Figure 2). All additional cytoskeletal immunohistochemistry were completely normal (data not shown).

Exclusion of Known Myopathies

Initial studies on index patients (50 and 11) with immunocytochemical staining and western blotting excluded the X-linked MDs (DMD, BMD, and EDMD), and numerous autosomal limb-girdle MDs (1C, 2I, 2B, 2C, 2D, 2E, and 2F). Myotonic dystrophies type 1 and 2, Kennedy syndrome, and McLeod myopathy were excluded by molecular-genetic analysis. Subsequently, a more detailed pedigree was established, and analysis suggested that this family displays a late-onset myopathy with X-linked recessive inheritance. To exclude the possibility that the phenotype in these cases is a variant form of DMD or BMD, we performed linkage analysis to the *DMD* locus by using five selected STRP intragenic markers at the *DMD* gene: DXS1238, DXS1237, DXS997, DXS1236, and DXS1235. Different haplotypes were revealed except for marker DXS1237 within our patients at the *DMD* locus, thereby excluding this locus as the causative gene in this family (Table 3). Subsequent screening for mutations in the *DMD* gene was conducted by sequencing patient's cDNA proximal to the first recombination event (including exons 1–44), thereby adding further weight to the exclusion of *DMD*. Thus, the *DMD* locus was ruled out by immunocytochemistry, indirect DNA analysis, and direct DNA analysis.

In order to exclude desminopathies, which share some of the phenotypic features observed in these two families, we performed immunocytochemical analysis for desmin, which was normal except in patient 11 (see Figure 1) who displays the clinically most advanced status of disease among the living family members. In his specimen of biopsied muscle, desmin staining showed reduced signal (data not shown).

Genetic Analysis

Genotypes for STRP markers across the X chromosome were analyzed. The threshold for statistically significant evidence of linkage of X-linked traits is $Z > 2.0$.[11] Two-point parametric LOD scores were calculated (DXS1047, 128.9 Mb, LOD = 2.4; DXS8094, 136.1 Mb, LOD = 3.3; DXS1192, 138.2 Mb, LOD = 3.4; and DXS1232, 139.1 Mb, LOD = 2.6; $\theta = 0$ [distances according to UCSC March 2006 freeze]; see Table 4 and Figure 3). Multipoint, nonparametric LOD scores were calculated, and gave a maximum LOD score of 2.4 around DXS8094 (Figure 3). Haplotype analysis was performed with CYRILLIC v2.1 (Cyrillic Software, UK) (data available on request from the authors [C.W.]). Recombination events in affected subjects and obligate carriers allowed us to determine a common disease haplotype. The distal boundary is defined by marker DXS1227 (140.6 Mb), and the proximal boundary is defined by marker DXS8055 (114.6 Mb), by recombination events in individual 20. Subsequently, we performed a genome-wide SNP genotype analysis (~250K; NspI Affymetrix chip) on five affected individuals, two obligate carriers, and one unaffected individual. Hemizygosity mapping with dChip software[10] confirmed a 12 Mb shared disease haplotype for all affected subjects and obligate carriers analyzed, on Xq25–q27.1, which encompasses 407 consecutive SNPs (rs4614130 [126.569 Mb, Xq25] to rs5907636 [138.561 Mb, Xq27.1]).

Mutation Screening of Candidate Genes

Four candidate genes that are from the Xq26–q27 critical region and that encode structural proteins expressed in

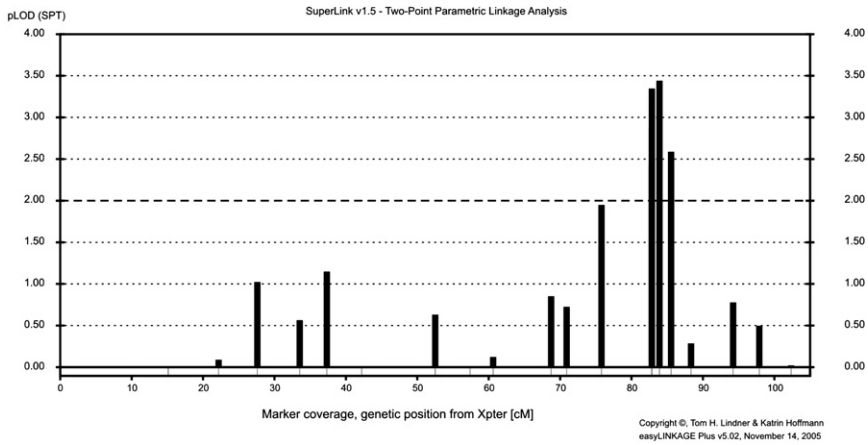

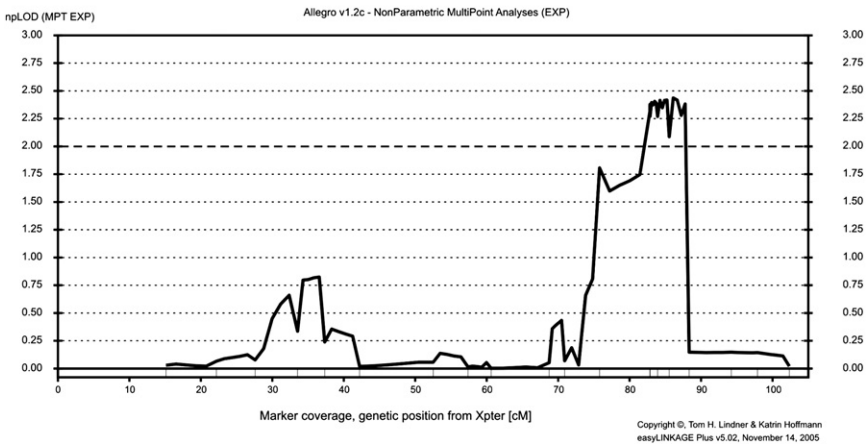

Figure 3. Two-Point Parametric and Multipoint Nonparametric Linkage Analysis for the XMPMA Family

Linkage data for X chromosome STRPs, analyzed with the SuperLink program version 1.5[9] from easyLINKAGE plus v5.02.[7] Allele frequencies were assumed to be equal, and disease frequency was set to 0.0001. Multipoint LOD scores were calculated with ALLEGRO version 1.2c.[8] Positions of markers are indicated in centimorgan (cM), as provided by Marshfield. Maximum LOD scores are shown.

muscle were screened. The muscleblind-like protein *3* (*MBNL3*), vestigial-like 1 (*VGLL1*), and fibroblast growth factor 13 (*FGF13*) genes were all sequenced from genomic DNA, but no coding mutations were identified. Sequencing of the four and a half LIM domain 1 gene (*FHL1*, NM_001449) identified a transversion at position 672 C → G leading to the amino acid substitution cysteine to tryptophan, C224W (Figures 4 and 5). This mutation cosegregated with disease status within the family; all six affected subjects were hemizygous, and all obligate carriers were heterozygous for the mutated allele. The mutation was not detected in 402 mixed European ancestry and 570 Austrian control chromosomes, and was not present either in published SNP databases or in published spliced expressed sequence tag (EST) sequences. In the UK family, mutation screening of *FHL1* identified a 3 bp insertion after nucleotide 381 (c.381_382insATC), leading to the insertion of an isoleucine residue within the second LIM domain (p.Phe127_Thr128insIle) (Figures 4 and 5). This mutation was not detected in 570 Austrian chromosomes and is not present in SNP databases.

Conservation Analysis

Box-shade alignment shows a high degree of conservation of amino acid sequence for FHL1, and for the fourth LIM domain in particular (Figure 4), across all vertebrate species. Conservation of cysteine residues is 100%. Also, the number of amino acid residues between cysteine residues is highly conserved, and at the location of the insertion mutation in the second LIM domain, there are two amino acids between the cysteine residues in all vertebrate species studied. This spacing appears to be a consistent feature of LIM-domain proteins. Homology is also high between the vertebrate FHL1 sequences and homologous sequences for nonvertebrates such as *C. elegans* and *Drosophila* (data not shown), and again, all cysteine residues are preserved, although sequences for these organisms might be more closely related to FHL2 and might thus represent an ancestral protein that later diverged into the different FHL proteins.

Western Analysis

Western blotting was performed a number of times, with anti-FHL1 antibody showing almost complete absence of the FHL1-protein band at 29 kDa in all patients compared to normal and disease (MD) controls (Figure 6). The FHL1 band showed similar strength in disease controls (LGMD and BMD) in comparison to healthy controls, thus implying that reduction of FHL1 protein is not a common feature of myopathy pathogenesis.

Immunohistochemical Analysis of FHL1

In skeletal muscle of normal controls, FHL1 staining revealed a checkered expression pattern. Fibers coexpressing slow myosin heavy chain showed relatively weak FHL1 expression, whereas many, but not all, fibers negative for slow myosin heavy chain showed higher FHL1 expression. This indicates that FHL1 is expressed in all muscle fibers, although higher levels are detected in a subset of fast-twitch muscle fibers. This pattern was identical in skeletal muscle of patients, although the staining intensity was lower (Figure 6).

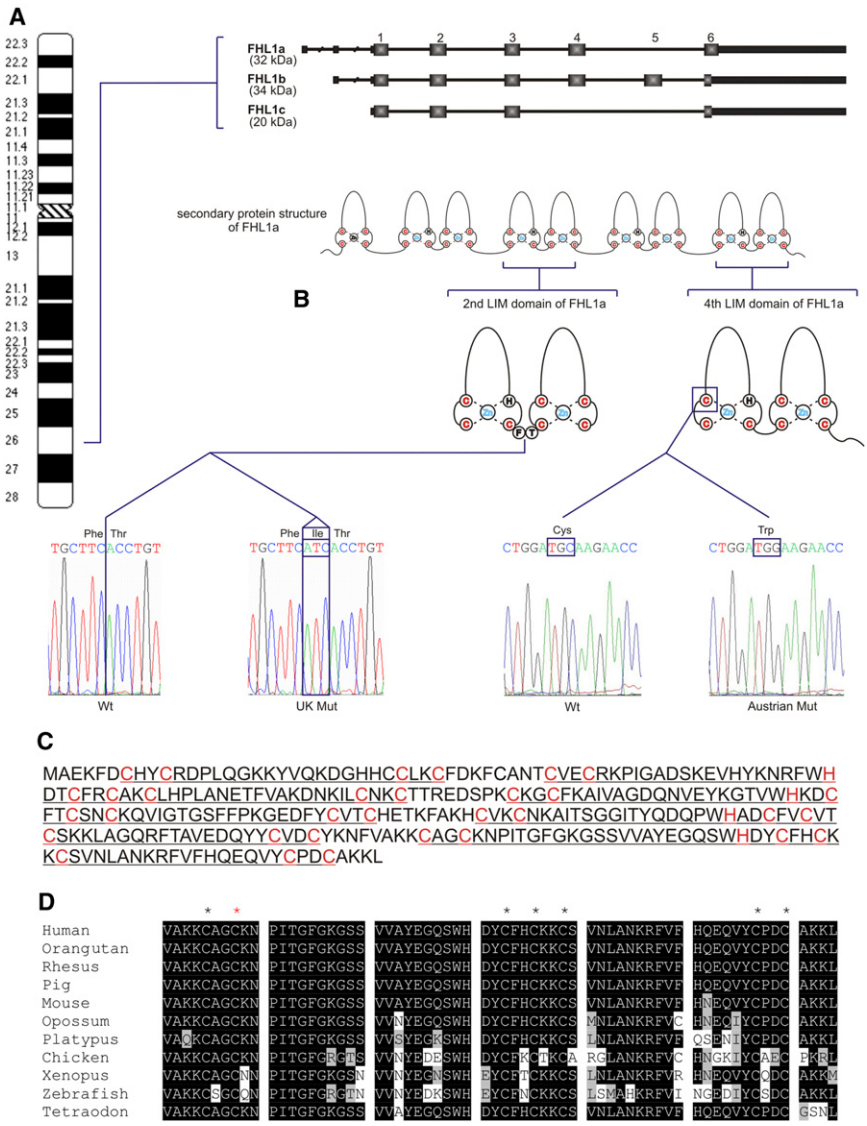

Figure 4. Ideogrammatic Representation of the XMPMA Locus on the Distal Arm of Chromosome X, Genomic Organization, Mutation Identification, and Protein Sequence of the FHL1 Gene

(A) The XMPMA locus on Xq26.3 is indicated, along with the intron/exon structure of FHL1 isoforms A, B, and C. Protein sizes (kDa) for the different isoforms were determined by western hybridization by Brown et al.[21] for FHL1a and by Ng et al.[22] for FHL1c.

(B) Electropherograms indicating the wild-type and mutation sequence for the Austrian and UK XMPMA families are shown, as well as the secondary structure of FHL1, indicating the position of the resulting amino acid substitution, C224W, relative to structural features in the protein.

(C) Amino acid sequence for FHL1a, indicating LIM domains that were underlined, and Zn^{2+}-binding cysteine residues were indicated in red type.

(D) Comparative analysis: Analysis of the amino acid sequence for fourth LIM domain of FHL1 across vertebrate species with BOXSHADE. Zn^{2+}-binding cysteine residues (*) and the position of mutation Cys224Trp (C224W) (*) are indicated. The domain and cysteine residues are highly conserved across vertebrates, from primates through to amphibians and primitive fish.

Immunohistochemistry of Primary Human Myoblasts

In keeping with the immunoblot results, staining of cultured, primary myoblasts of patient 50 for FHL1 revealed a reduction of overall expression, but no overt aberration of subcellular localization, as compared to normal controls (Figure 7). In both, patient and control myoblasts FHL1 was expressed primarily in the cytoplasm.

Discussion

A new and phenotypically distinct X-linked myopathy, XMPMA, has been described in this study, with the main clinical presentation being atrophy of postural muscles combined with a generalized hypertrophy. Although it is clinically distinct, the possibility that the disorder might be an allelic form of a known X-linked myopathy was ruled out by a combination of immunohistochemical and genetic studies; X-linked myopathies excluded are DMD, BMD, EDMD, and XMEA and also McLeod syndrome, Barth syndrome (Xq28; MIM #302060), and myotubular myopathy 1 (MTM1; Xq28; MIM #310400). Linkage studies and haplotype analysis led to the identification of the Xq25–q27.1 region for the XMPMA locus, and four functional candidate genes were selected from within this region and were screened for possible disease-related mutations. *FHL1* on Xq26.3 was found to have the amino acid substitution C224W segregating with disease in the Austrian family. Analysis of the protein by western blotting with FHL1-specific antibodies indicated a striking reduction of FHL1 levels in patients' muscle cells, apparently corroborating the genetic findings. FHL1 protein, however, was not reduced in muscle tissue from patients with either Becker or LGMD, suggesting that reduction of FHL1 is not a common feature among myopathies.

FHL1 is expressed in skeletal and cardiac muscle, is more abundant in oxidative fibers (as shown in rat studies[12]), and is suggested to play a role in sarcomere synthesis and assembly.[13] FHL1 has been shown to be involved in regulation of muscle fiber type I development in fish.[14] FHL1 is a member of LIM-only proteins, containing four and a half LIM domains (named from the initials of the first three homeodomain proteins in which it was discovered: LIN11, ISL1, and MEC3[15]) with the FHL-specific LIM

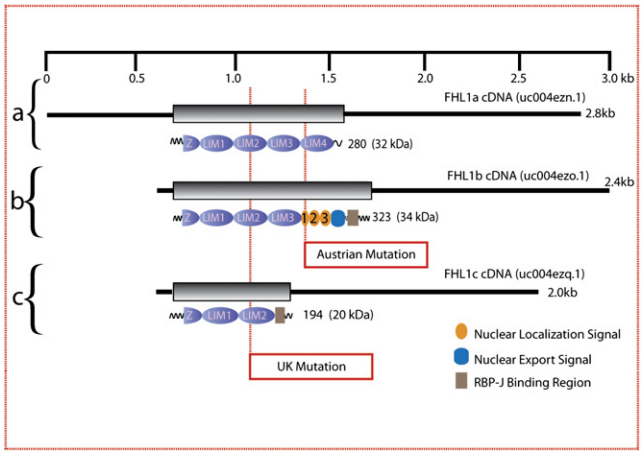

Figure 5. Isoforms of FHL1
The organization of tandem LIM domains, as well as nuclear localization signals, nuclear export signals, and protein binding domains for FHL1 isoforms A, B, and C are shown. The cDNA and protein for each isoform are displayed alongside each other, with cDNA size and the number of amino acids present in each isoform being indicated on the right-hand side. The positions of the mutations in the Austrian family (p.C224W) and UK family (p.F127_T128insI) are shown relative to the three different FHL1 isoforms.

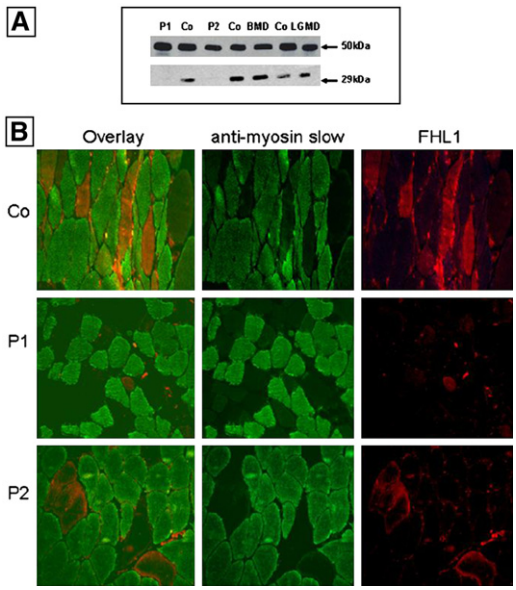

Figure 6. Western Blot and FHL1/Myosin Slow Immunofluorescence
(A) FHL1 western blotting: In specimens from patients 50 and 11 (P1 and P2), a normal control (Co), and controls with either Becker MD (BMD) or limb girdle MD (LGMD), the specific FHL1 band at 29 kDa is severely reduced compared to normal and disease controls. The 50 kDa band corresponds to alpha-sarcoglycan (adhalin) showing equal quantity of protein loading in all samples.
(B) Anti-FHL1 and anti-myosin slow-type immunofluorescence of human muscle from two patients with FHL1 mutation. The top row shows control samples: Overlay shows that FHL1 (red) does not colocalize to myosin slow type (green). Shown in the middle row: An overlay in a patient with FHL1 mutation reveals nearly complete loss of FHL1 staining. Shown in the bottom row: Overlay in a patient with FHL1 mutation shows a very few remaining anti-FHL1-positive fibers.

consensus sequence C-X_2-C-X_{16-21}-H-X_2-C-X_2-C-X_2-C-X_{17}-C-X_2-C. LIM domains are cysteine rich, double-zinc binding structures consisting of two subdomains, each responsible for binding one Zn^{2+} ion. Metal ions are known to stabilize the tertiary conformation of proteins. Thus, the zinc ions help define the tertiary structure of the LIM domain and thereby generate a binding interface for proteins.[16] The C224W mutation replaces a highly conserved cysteine within the fourth LIM domain of FHL1, which is one of the four cysteines needed for the central binding of a Zn^{2+} ion (Figure 4). Mutations at conserved cysteines that are involved in zinc binding have been shown to have a highly deleterious effect on the tertiary structure of the protein.[17] In vitro mutagenesis studies of conserved Zn^{2+}-binding cysteines within LIM domains have demonstrated that substitution results in diminished Zn^{2+}-coordination and might eliminate the stability of the LIM tertiary structure.[18] Furthermore, in the progressive neurodegenerative disorder Mohr-Tranebjaerg syndrome (MIM #304700), a disease-causing cysteine-to-tryptophan substitution within a Cys4 metal-binding motif of the DDP1/TIMM8A gene was shown to ablate Zn^{2+} binding.[19] In the muscle LIM protein (MLP or CSRP3), which is known to be causative for hypertrophic cardiomyopathy (CMD1M; MIM #607482), mutation of a Zn^{2+}-coordinating cysteine residue completely ablates the Zn^{2+} binding for the second zinc finger within the first LIM domain. This leads to the protein being more unstable and vulnerable to proteolysis, as well as reducing its protein-protein interactions.[20] Thus, it is very likely that mutations affecting the Zn^{2+}-complexing property of FHL1 cause hypertrophy of skeletal as well as cardiac muscles, analogous to the situation with MLP causing hypertrophy of cardiac muscle in HCM. The UK mutation results in the insertion of an isoleucine residue between the two amino acid residues (127 to 128) that link the two Zn^{2+} fingers of the second LIM domain and is likely to disrupt the protein conformation. The consensus C-X_2-C spacing of the subdomains in

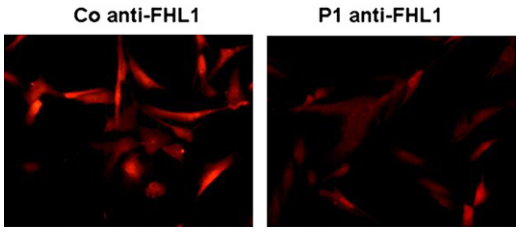

Figure 7. Expression Analysis of FHL1 in Primary Human Myoblasts
Anti-FHL1 staining in primary myoblasts from control (Co) and from patient 50 (P1). The patient's myoblasts show lower expression of FHL1, but subcellular distribution is not different to control. Both patient and control show primarily cytoplasmic but also nuclear FHL1 distribution.

LIM proteins is highly conserved across evolution. Thus, the altered distance between the two Zn^{2+} finger subdomains is expected to have an adverse effect on the protein-protein binding properties of the LIM domain.

FHL1 has at least three different isoforms, which differ in their amino acid sequence, expression pattern, binding partners, and subcellular localization: isoform A (FHL1A, SLIM1, and Q13642-1 [ExPASy number]) is abundantly expressed, with highest levels in skeletal muscle, and intermediate expression in heart, and low-level expression in placenta, ovary, prostate, testis, small intestine, and colon; isoform B (FHL1B, SLIMMER, and Q13642-2) is abundantly expressed in skeletal muscle, with lower expression in heart, colon, prostate, and small intestine (from Northern hybridization analysis[21]); and isoform C (FHL1C and Q13642-3) is expressed at much lower levels compared to FHL1A, in testis, heart, and skeletal muscle (from Northern hybridization analysis[22]).

The C224W mutation affects FHL1 isoforms A (the most prevalent isoform[22]) and B but not C. The isoleucine insertion mutation in the UK family affects all three isoforms. FHL1A and FHL1B are identical until amino acid residue 230, beyond which alternative splicing results in the fourth LIM domain being replaced by sequences for nuclear/cytoplasmic shuttling and transcription-factor binding in FHL1B (Figure 5). Thus, the functional consequences of C224W on FHL1A and FHL1B are expected to be different: Whereas C224W is likely to disrupt the Zn^{2+}-binding properties of FHL1A, in FHL1B, the mutation is located within the first nuclear localization sequence (NLS1) and thus might result in impaired FHL1B shuttling between nucleus and cytoplasm.[21] A number of protein binding partners, including myosin-binding proteins MYBPC1 (slow type) and MYBPC3 (cardiac), as well as SRF and ERK2, bind to different LIM domains within FHL1. Mutations in MYBPC3 are the second most common cause of familial hypertrophic cardiac myopathy.[23,24] FHL1 is considered to be a regulator of MYBPC activity and thus involved in sarcomere assembly.[12] As a result of the different protein-binding properties of the different LIM domains in FHL1, mutations within the different domains might have different phenotypic consequences. Another MYBPC1 binding partner is deleted in muscular dystrophy Ky knockdown mice, which display myopathy with postural-muscle weakness that leads to kyphoscoliosis and that results in a shift from fiber type 2 to 1.[25] Interestingly, in contrast to the XMPMA patients, there is no evidence of hypertrophy in these mice. We hypothesize that the two MYBPC1-binding partners, Ky and FHL1, determine the composition of muscle fibers in skeletal muscles, and dysregulation might lead to myopathies affecting postural muscles.

Involvement of axial muscles, rigidity of the spine, and ankle contractures are prominent symptoms in a number of skeletal muscle disorders such as selenoprotein 1, Lamin A/C, and collagen-6-related myopathies.[26] However, muscle hypertrophy is not a common feature in these disorders. Recently, desmin mutations were identified in patients with a scapuloperoneal myopathy with axial muscle weakness.[27] The desmin protein accumulation detected in muscle fibers of *FHL1*-mutated patients might suggest a similar pathophysiological pathway as in desmin-related myopathies.

In summary, we have identified the gene *FHL1*, and its encoded protein, as responsible for a new form of X-linked recessive myopathy termed XMPMA. The phenotypic features described in the Austrian and UK families, in particular the specific atrophy of postural muscles and pseudoathleticism, might be specific for mutations within the SRF and MyBPC1 (muscle fiber type 1-specific isoform) and ERK2-binding regions of FHL1. FHL1 is most likely to be a modulator of skeletal muscle hypertrophy, as is the case for FHL2 and CSRP3 in cardiac hypertrophy.[28] We hypothesize that mutations elsewhere in the gene are likely to result in a more heterogeneous myopathic phenotype because of the binding-partner specificity of the different LIM domains in FHL1, as well as the isoform-specificity of various domains within FHL1. This has considerable implications for diagnostic evaluation, screening, and genetic counseling of patients (also carriers) with myopathy of unknown genetic cause, particularly in cases such that pedigree information would suggest X-linked inheritance, but the Becker and Duchenne MD, Emery-Dreifuss MD, XMEA, and McLeod are excluded. In addition, it has been noted that cardiomyopathy is present in at least four affected members of the large XMPMA family, and thus the *FHL1* gene might also be a strong candidate for hereditary and sporadic cardiomyopathy.

Acknowledgments

We wish to express our gratitude to the patients and their families for participating in this study. We thank Ursula Klutzny and Maria Schmuck (Munich), Ingrid Janisch and Michaela Loibner-Pommer (Graz), and The Centre for Applied Genomics (www.tcag.ca), and Chao Lu in particular, for technical assistance. C.W. is supported by a postdoctoral fellowship from the Centre for Addiction and Mental Health, Toronto. J.B.V. is supported by an Early Researcher Award from the Ontario Ministry of Research. B.S., V.S., and H.L. are members of the German Muscular Dystrophy Network (*MD-NET* 01GM0601) funded by the German Ministry of Education and Research (BMBF, Bonn, Germany); www.md-net.org. *MD-NET* is a partner of TREAT-NMD (EC, 6th FP, proposal #036825; www.treat-nmd.eu).

Received: June 26, 2007
Revised: August 21, 2007
Accepted: September 17, 2007
Published online: January 10, 2008

Web Resources

The URLs for data presented herein are as follows:

Boxshade, http://bioweb.pasteur.fr/seqanal/interfaces/boxshade.html
dChip, http://www.dchip.org
ExPASy, http://expasy.org/sprot/
Online Mendelian Inheritance in Man (OMIM), http://www.ncbi.nlm.nih.gov/Omim

Primer3, http://frodo.wi.mit.edu/cgi-bin/primer3/primer3_www.cgi
UCSC Genome Browser, http://genome.ucsc.edu

References

1. Davies, K.E., and Nowak, K.J. (2006). Molecular mechanisms of muscular dystrophies: Old and new players. Nat. Rev. Mol. Cell Biol. *7*, 762–773.
2. Ellis, J.A. (2006). Emery-Dreifuss muscular dystrophy at the nuclear envelope: 10 years on. Cell. Mol. Life Sci. *63*, 2702–2709.
3. Kalimo, H., Savontaus, M.-L., Lang, H., Paljarvi, L., Sonninen, V., Dean, P.B., Katevuo, K., and Salminen, A. (1988). X-linked myopathy with excessive autophagy: A new hereditary muscle disease. Ann. Neurol. *23*, 258–265.
4. Danek, A., Rubio, J.P., Rampoldi, L., Ho, M., Dobson-Stone, C., Tison, F., Symmans, W.A., Oechsner, M., Kalckreuth, W., Watt, J.M., et al. (2001). McLeod neuroacanthocytosis: Genotype and phenotype. Ann. Neurol. *50*, 755–764.
5. Schwarzmeier, J., Moser, K., and Lujf, A. (1971). Pyruvate kinase deficiency of erythrocytes in a case of hereditary myopathy. Klin. Wochenschr. *49*, 156–158.
6. Dubowitz, V., and Sewry, C.A. (2007). Muscle Biopsy: A Practical Approach, Third Edition (Edinburgh: Sanders/Elsevier).
7. Lindner, T.H., and Hoffmann, K. (2005). easyLINKAGE: A PERL script for easy and automated two-/multi-point linkage analyses. Bioinformatics *21*, 405–407.
8. Gudbjartsson, D.F., Jonasson, K., Frigge, M.L., and Kong, A. (2000). Allegro, a new computer program for multipoint linkage analysis. Nat. Genet. *25*, 12–13.
9. Fishelson, M., and Geiger, D. (2002). Exact genetic linkage computations for general pedigrees. Bioinformatics *18* (*Suppl 1*), S189–S198.
10. Li, C., and Wong, W.H. (2001). Model-based analysis of oligonucleotide arrays: Expression index computation and outlier detection. Proc. Natl. Acad. Sci. USA *98*, 31–36.
11. Ott, J. (1991). Analysis of Human Genetic Linkage (Baltimore: Johns Hopkins University Press)., pp. 65.
12. Loughna, P.T., Mason, P., Bayol, S., and Brownson, C. (2000). The LIM-domain protein FHL1 (SLIM 1) exhibits functional regulation in skeletal muscle. Mol. Cell Biol. Res. Commun. *3*, 136–140.
13. McGrath, M.J., Cottle, D.L., Nguyen, M.A., Dyson, J.M., Coghill, I.D., Robinson, P.A., Holdsworth, M., Cowling, B.S., Hardeman, E.C., Mitchell, C.A., et al. (2006). Four and a half LIM protein 1 binds myosin-binding protein C and regulates myosin filament formation and sarcomere assembly. J. Biol. Chem. *281*, 7666–7683.
14. Chauvigné, F., Cauty, C., Ralliére, C., and Rescan, P.Y. (2005). Muscle fiber differentiation in fish embryos as shown by in situ hybridization of a large repertoire of muscle-specific transcripts. Dev. Dyn. *233*, 659–666.
15. Freyd, G., Kim, S.K., and Horvitz, H.R. (1990). Novel cysteine-rich motif and homeodomain in the product of the Caenorhabditis elegans cell lineage gene lin-11. Nature *344*, 876–879.
16. Michelsen, J.W., Schmeichel, K.L., Beckerle, M.C., and Winge, D.R. (1993). The LIM motif defines a specific zinc-binding protein domain. Proc. Natl. Acad. Sci. USA *90*, 4404–4408.
17. Taira, M., Otani, H., Saint-Jeannet, J.P., and Dawid, I.B. (1994). Role of the LIM class homeodomain protein Xlim-1 in neural and muscle induction by the Spemann organizer in Xenopus. Nature *372*, 677–679.
18. Michelsen, J.W., Sewell, A.K., Louis, H.A., Olsen, J.I., Davis, D.R., Winge, D.R., and Beckerle, M.C. (1994). Mutational analysis of the metal sites in an LIM domain. J. Biol. Chem. *269*, 11108–11113.
19. Hofmann, S., Rothbauer, U., Muhlenbein, N., Neupert, W., Gerbitz, K.D., Brunner, M., and Bauer, M.F. (2002). The C66W mutation in the deafness dystonia peptide 1 (DDP1) affects the formation of functional DDP1.TIM13 complexes in the mitochondrial intermembrane space. J. Biol. Chem. *277*, 23287–23293.
20. Geier, C., Perrot, A., Ozcelik, C., Binner, P., Counsell, D., Hoffmann, K., Pilz, B., Martiniak, Y., Gehmlich, K., van der Ven, P.F., et al. (2003). Mutations in the human muscle LIM protein gene in families with hypertrophic cardiomyopathy. Circulation *107*, 1390–1395.
21. Brown, S., McGrath, M.J., Ooms, L.M., Gurung, R., Maimone, M.M., and Mitchell, C.A. (1999). Characterization of two isoforms of the skeletal muscle LIM protein 1, SLIM1. Localization of SLIM1 at focal adhesions and the isoform slimmer in the nucleus of myoblasts and cytoplasm of myotubes suggests distinct roles in the cytoskeleton and in nuclear-cytoplasmic communication. J. Biol. Chem. *274*, 27083–27091.
22. Ng, E.K., Lee, S.M., Li, H.Y., Ngai, S.M., Tsui, S.K., Waye, M.M., Lee, C.Y., and Fung, K.P. (2001). Characterization of tissue-specific LIM domain protein (FHL1C) which is an alternatively spliced isoform of a human LIM-only protein (FHL1). J. Cell. Biochem. *82*, 1–10.
23. Watkins, H., Conner, D., Thierfelder, L., Jarcho, J.A., MacRae, C., McKenna, W.J., Maron, B.J., Seidman, J.G., and Seidman, C.E. (1995). Mutations in the cardiac myosin binding protein-C gene on chromosome 11 cause familial hypertrophic cardiomyopathy. Nat. Genet. *11*, 434–437.
24. Carrier, L., Bonne, G., Bahrend, E., Yu, B., Richard, P., Niel, F., Hainque, B., Cruaud, C., Gary, F., Labeit, S., et al. (1997). Organization and sequence of human cardiac myosin binding protein C gene (MYBPC3) and identification of mutations predicted to produce truncated proteins in familial hypertrophic cardiomyopathy. Circ. Res. *80*, 427–434.
25. Blanco, G., Coulton, G.R., Biggin, A., Grainge, C., Moss, J., Barrett, M., Berquin, A., Marechal, G., Skynner, M., van Mier, P., et al. (2001). The *kyphoscoliosis* (*ky*) mouse is deficient in hypertrophic responses and is caused by a mutation in a novel muscle-specific protein. Hum. Mol. Genet. *10*, 9–16.
26. Mendell, J.R., Boue, D.R., and Martin, P.T. (2006). The congenital muscular dystrophies: Recent advances and molecular insights. Pediatr. Dev. Pathol. *9*, 427–443.
27. Walter, M.C., Reilich, P., Huebner, A., Fischer, D., Schroder, R., Vorgerd, M., Kress, W., Born, C., Schoser, B.G., Krause, K.H., et al. (2007). Scapuloperoneal syndrome type Kaeser and a wide phenotypic spectrum of adult-onset, dominant myopathies are associated with the desmin mutation R350P. Brain *130*, 1485–1496.
28. Kong, Y., Shelton, J.M., Rothermel, B., Li, X., Richardson, J.A., Bassel-Duby, R., and Williams, R.S. (2001). Cardiac-specific LIM protein FHL2 modifies the hypertrophic response to betaadrenergic stimulation. Circulation *103*, 2731–2738.
29. Johnson, M.A., Sideri, G., Weightman, D., and Appleton, D. (1973). A comparison of fibre size, fibre type constitution and spatial fibre type distribution in normal human muscle and in muscle from cases of spinal muscular atrophy and from other neuromuscular disorders. J. Neurol. Sci. *20*, 345–361.